RESEARCH PAPER | Engineering | Volume : 4 | Issue : 2 | Feb 2014 | ISSN - 2249-555X

Simulation Possibilities Concerned to Thermocouple Response Related to Flowing Media Temperature Step Change with the Use of CFD Method

KEYWORDS: Thermocouple, CFD simulations, heat transport, thermocouple response, turbulent model

Ludovit Medvecky
Associate Professor, Department of Design and Mechanical Element, Faculty of Mechanical Engineering, University of Žilina, Univerzitná 8215/1, 010 26 Žilina, Slovakia

Jan Labaj
Associate Professor, Dubnica Technological Institute, Sládkovičova 533/20, 018 41 Dubnica nad Váhom, Slovakia

Peter Schutz
Ing. (Ingenieur - Master of Science in Engineering equivalent), Embraco Slovakia, Spišská Nová Ves, Slovakia

Dusan Repcik
Professor, University of Security Management in Košice, Košice, Slovakia

ABSTRACT *The paper deals with possibilities of verification, which is concerned to effect of protective cover and thermocouple body related to response speed with the use of CFD (Computational Fluid Dynamics) Method. However, the paper contains a description concerned to step rise of temperature within thermocouple measuring area depending on gas temperature step change, while that is flowing off the thermocouple as well. A selection of an appropriate turbulence model together with an adequate bordering layer enables applying calculations in order to simulate different arrangement and number of holes within thermocouple protective pipe.*

INTRODUCTION

The thermocouples play a role of great importance, in a technical practice, as sensors when measuring temperature values. Their design and allocation within protective pack have a direct influence related to their response speed. When applying the thermocouple in order to provide a temperature measurement concerned to flowing media that shall contain a protective cover or pack with adequate number of holes, which enable an appropriate media access. The above-mentioned protective pack has a direct effect related to thermocouple response speed via its own thermal capacity, density and thermal conductivity (temperature coefficient) and via flowing of media round the thermocouple body as well.

The sensor operating based on a thermocouple element is considered to be the most suitable for temperature measurement, which may have at about 1000oC and their flow speed may achieve up to 60m.s^{-1}. However, there shall be considered further important aspects like, precision, price, dimensions or consumption of energy as well.

As a result of that, the above-mentioned types of sensors are mostly applied for these purposes, however there may also exist different type of construction or designs based on different types of materials.

Theoretical aspects

The following continuity equation may postulated for quantitative description of gas, which is considered to be viscous, supersonic, and compressible, indicating two dimensional flow with no chemical reactions and respecting ideal gas features ($\gamma = c_p/c_v$) – see also formula (1). However, further important assumptions shall be postulated in order to confirm formula (1) validity and they may be defined as follows:

- Parallel and perpendicular orientation of Cartesian co-ordinates x and y, while the orientation is the same like the gas flow.
- The symbols u and v represent speeds in the same directions like x and y co-ordinates

$$\frac{\partial \rho}{\partial t} + \frac{\partial \rho u}{\partial x} + \frac{\partial \rho v}{\partial y} = 0. \quad (1)$$

On the other hand, the co-ordinate x quantity of motion values are defined via formula (2) and the co-ordinate y quantity of motion values are defined via formula (3), while the energy or power balance relations may be quantified via equation (4)

$$\frac{\partial \rho u}{\partial t} + \frac{\partial \rho u^2}{\partial x} + \frac{\partial \rho u v}{\partial y} + \frac{\partial p}{\partial x} - \frac{\partial \tau_x}{\partial x} - \frac{\partial \tau_{yx}}{\partial y} = 0, \quad (2)$$

$$\frac{\partial \rho v}{\partial t} + \frac{\partial \rho u v}{\partial x} + \frac{\partial \rho v^2}{\partial y} + \frac{\partial p}{\partial y} - \frac{\partial \tau_{yx}}{\partial x} - \frac{\partial \tau_y}{\partial y} = 0, \quad (3)$$

$$\frac{\partial \rho E}{\partial t} + \frac{\partial \rho E u}{\partial x} + \frac{\partial \rho E v}{\partial y} - \nabla . \vec{q} + p \nabla . \vec{v} - \phi = 0 \quad (4)$$

If the system copies the ideal gas status and is represented via ideal gas status equation $p = \rho R T$ and the total energy value may be calculated based on formula $E = cv T$, a set of appropriate shearing stress components may be postulated via formulas (5, 6 and 7).

$$\tau_x = \lambda \nabla . \vec{v} + 2\mu \frac{\partial u}{\partial x}, \quad (5)$$

$$\tau_{yx} = \tau_x = \mu \left(\frac{\partial v}{\partial x} + \frac{\partial u}{\partial y} \right), \quad (6)$$

$$\tau_y = \lambda \nabla . \vec{v} + 2\mu \frac{\partial v}{\partial y}, \quad (7)$$

The next equation (8) contains thermal conductivity coefficient $\lambda = -2/3$, which is going out from Stokes hypothesis and the items contained in equations (8, 9) are postulated as follows: μ – dynamic viscosity, T-temperature, R – ideal gas constant, p – pressure and c_v – thermal capacity at the constant volume.

The thermal flow is expressed via equation (8)

Volume : 4 | Issue : 2 | Feb 2014 | ISSN - 2249-555X

$$\nabla . \vec{q} = \nabla . k \nabla T = \frac{\partial}{\partial x}\frac{(k \partial T)}{\partial x} + \frac{\partial}{\partial y}\frac{(k \partial T)}{\partial y} \quad (8)$$

and dissipating function Φ is

$$\Phi = (\lambda \nabla . \vec{v}) \left(\frac{\partial u}{\partial x} + \frac{\partial v}{\partial y} \right) + \quad (9)$$

$$+ 2\mu \left[\left(\frac{\partial u}{\partial x} \right)^2 + \left(\frac{\partial v}{\partial y} \right)^2 \right] + \left(\frac{\partial u}{\partial y} + \frac{\partial v}{\partial x} \right)^2 .$$

The molecular viscosity is being postulated via Sutherland's law

$$\frac{\mu}{\mu_\infty} = \left(\frac{T}{T_\infty} \right)^{3/2} \frac{T_\infty + S}{T + S}, \quad (10)$$

where S is considered to be the Sutherland's constant.

$$\frac{k}{k_\infty} = \frac{\mu}{\mu_\infty}. \quad (11)$$

The FVM – finite volume method is applied, when looking for a solution of the above-mentioned equations.

FVM - finite volume method

The fluid flowing space consists of a small volume final number. The mass, motivity and energy transfer values are being calculated for each of the above-mentioned volumes. The Euler's equations (see also formula 12) may have an integral form or shape, while that shape represents an example and is used for explanation purposes.

$$\frac{\partial}{\partial t} \int_{\Delta R} \int U \, dx \, dy + \int_R [F.dy - G.dx] = 0, \quad (12)$$

while ΔR is considered to be the flow domain, R is the flow border, x and y are considered to be Cartesian's coordinates The U, F and G vectors, which create an integral part of equation (13) are considered to be x and y direction speed components

$$U = \begin{bmatrix} \rho \\ \rho u \\ \rho v \\ \rho E \end{bmatrix}, \quad F = \begin{bmatrix} \rho u \\ \rho u^2 + p \\ \rho u v \\ \rho u H \end{bmatrix}, \quad G = \begin{bmatrix} \rho v \\ \rho u v \\ \rho v^2 + p \\ \rho v H \end{bmatrix}, \quad (13)$$

in equations (13), ρ – is the density, u, v – speed components related x and y, p- pressure, E represents the total energy and H- represents the total enthalpy.

When considering ideal gas the formulas (14) a (15) where the formula $\gamma = c_p/c_v$ represents the specific heat ratio.

$$E = \frac{p}{(\gamma - 1)\rho} + \frac{1}{2}(u^2 + v^2), \quad (14)$$

$$H = E + \frac{p}{\rho}, \quad (15)$$

The method of final volumes in conservative form is considered to be a result of equation (12) approximation, while this task solution is based on integration scheme postulated by Runge Kutt.

Runge Kutt integration method

The flow domain consists of several small final volumes, while numeric approximation method related to equation (16) is being applied extra for each volume. An appropriate system of differential equations is considered to be a result of the above-mentioned procedure (see also equation 16).

$$\frac{d}{dt}[U \Delta A] + \tilde{Q} U - \tilde{D} U = 0, \quad (16)$$

A solution of these equations may be done with the use of many integration schemas, while the items contained within equation (16) are postulated as follows: ΔA – the element surface, $Q^{\sim}$ - space differential operator and $D^{\sim}$ is an artificial added disparity item which prevents a numeric instability, which may be observed within areas with rapid streaming changes. When applying the previous equation to an appropriate component related to quantity of motion, while the simplification disparity item may be neglected, the entire equation may have a shape of formula (17).

$$\frac{d}{dt}[\rho u . \Delta A] + \sum_{k=1}^{4} (\tilde{Q}_k \rho u_k + \Delta y_k \; p_k) = 0 \quad (17)$$

where the flowing speed may be postulated via formula (18), while the sum is concerned to all walls of the element.

$$Q_k = \Delta y_k u_k - \Delta x_k v_k \quad (18)$$

When looking at Fig.1, you can see for walls, which create an integral part of (i, j) element and are denoted as 1, 2, 3 and 4. The variables ρ, ρu, ρv, etc. are located in the middle and the values $(\rho U)_k$ are considered to be average values for all elements.

$$(\rho u)_1 = \frac{1}{2}\left[(\rho u)_{i,j} + (\rho u)_{i,j-1} \right] \quad (19)$$

$$(\rho u)_2 = \frac{1}{2}\left[(\rho u)_{i,j} + (\rho u)_{i+1,j} \right]$$

$$\Delta x_1 = (x_D - x_A)\tilde{i} \; ; \; \Delta y_2 = (y_C - y_D)\tilde{j},$$

In most cases, the equation (19) is being integrated with the use of scheme with four steps postulated by Runge Kutt, while the dispatching item is the same like in the first step. The values related to time level t will be applied in order to calculate a set of appropriate values concerned to t+1 time level, while the calculation process is being done in four phases (see also formula 19a)

$$U^{(1)} = U^t - \frac{\Delta t}{\Delta A}[\tilde{Q} U^t - \tilde{D} U^t],$$

$$U^{(2)} = U^t - \frac{\Delta t}{\Delta A}[\tilde{Q} U^{(1)} - \tilde{D} U^t], \quad (19a)$$

$$U^{(3)} = U^t - \frac{\Delta t}{\Delta A}[\tilde{Q} U^{(2)} - \tilde{D} U^t],$$

$$U^{t+1} = U^t - \frac{\Delta t}{\Delta A}[\tilde{Q} U^{(3)} - \tilde{D} U^t].$$

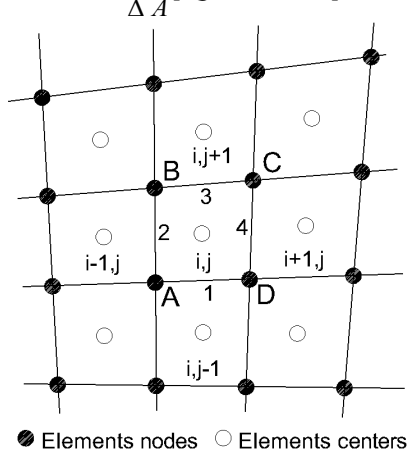

Figure 1: An example of two-dimensional calculating grid

Many turbulent models exist, which may be applied for these purposes, however a model based on two equations, denoted as k - ε RNG model was chosen in order to simulate generating whirling path, after the body to be investigated and find a relation concerned to aerodynamic thermocouple eclipse.

Volume : 4 | Issue : 2 | Feb 2014 | ISSN - 2249-555X

κ – ε MODEL BASED ON TWO EQUATIONS

The model based on two equations determines a length measure, which describes energy amount within large whirling's, while that determination is done via the second transport equation. This model is considered to be the subject of transport related to historical processes, while this is something similar like kinetic energy k. There may be postulated one example, where the whirling's generated by grid are carried away in a flow direction and the whirling size depends on their original size. On the other hand, the dissipating represents further process, which has an influence related to the length measure. Equilibrium among these processes may be quantified via model transport equation. However, the length distribution may be quantified via model transport equation as well. The dissipating speed ε also is considered the equation variable and may be calculated via formula (20).

$$\varepsilon = \frac{C_D k^{3/2}}{l} \qquad (20)$$

However, there is one difference, when comparing it with that equation, which is defined directly, no supplementary items shall be defined for speed measure l, in the case of streaming near the wall. The κ–ε model operates with Boussinesq's hypothesis which deal with whirling viscosity and there is a relation between v_t and k and v_t and C_μ, with respect to Kolmogor – Prandtl's formula postulated as $v_t = C_v k^{1/2} l$. With respect to that formula, the formula (21) may be postulated.

$$v_t = C_\mu \frac{k^2}{\varepsilon} \qquad (21)$$

The k –distribution is given via transport equation, however the dissipating item is being expressed via ε value. However, the formula, which represents an exact version of transport equation, may be derived based on Navier-Stokes equations as well. This equation contains a set of complex correlations, which shall be modeled again.

– the variables containing band signs are considered to the average values, where the time value, plays a role of principle importance)

$$\frac{\partial \varepsilon}{\partial t} + \frac{\partial \overline{u_j}\varepsilon}{\partial x_j} = \frac{\partial}{\partial x_j}\left(\frac{v_t}{\sigma_\varepsilon}\frac{\partial \varepsilon}{\partial x_j}\right) + c_{1\varepsilon} v_t \left(\frac{\partial \overline{u_j}}{\partial x_l} + \frac{\partial \overline{u_l}}{\partial x_j}\right)\frac{\partial \overline{u_l}}{\partial x_j} - c_{2\varepsilon}\frac{\varepsilon^2}{k} \quad (22)$$

STANDARD κ–ε MODEL

When applying that model, the solution of the following equation shall be found. For continuity equation (see also formula 23)

$$\frac{\partial \rho}{\partial t} + \frac{\partial}{\partial x_j}\left(\rho \overline{u_j}\right) = 0. \qquad (23)$$

Equation for transfer related to quantity of motion (see also formula 24)

$$\frac{\partial}{\partial t}\left(\rho \overline{u_l}\right) + \frac{\partial}{\partial x_j}\left(\rho \overline{u_l u_j}\right) = \qquad (24)$$

$$= \frac{\partial}{\partial x_j}\left[\mu_r\left(\frac{\partial \overline{u_i}}{\partial x_j} + \frac{\partial \overline{u_j}}{\partial x_i}\right) - \left(\frac{2}{3}\mu_r \frac{\partial \overline{u_l}}{\partial x_l}\right)\right] - \frac{\partial p}{\partial x_i} + \rho g_i + F_i$$

Equation for heat transfer (see also formula 25)

$$\frac{\partial}{\partial t}\left(\rho \overline{h}\right) + \frac{\partial}{\partial x_j}\left(\rho \overline{u_j h}\right) = \frac{\partial}{\partial x_j}\left(\lambda_t \frac{\partial \overline{T}}{\partial x_j}\right) + \frac{d\overline{p}}{dt} + \frac{\partial\left(\tau_J \overline{u_j}\right)}{\partial x_l} \qquad (25)$$

where λ_t effective thermal conductivity, which is observed as a result of turbulent transport.

Equation for transfer of turbulent kinetic energy k (see also formula 26)

$$\frac{\partial}{\partial t}\left(\rho k\right) + \frac{\partial}{\partial x_j}\left(\rho \overline{u_j} k\right) = \frac{\partial}{\partial x_j}\frac{\mu_t}{\sigma_k}\frac{\partial k}{\partial x_j} + P + G - \rho \qquad (26)$$

$$P = \mu_t\left[\frac{\partial \overline{u_j}}{\partial x_l}\frac{\partial \overline{u_l}}{\partial x_j}\right]\frac{\partial \overline{u_j}}{\partial x_l}, G = -g_j \cdot \frac{\mu_t}{\sigma_h}\frac{\partial \rho}{\partial x_j} \qquad (27)$$

Equation for dissipating speed ε: (see also formula 28)

$$\frac{\partial}{\partial t}\left(\rho\varepsilon\right) + \frac{\partial}{\partial x_j}\left(\rho \overline{u_j}\varepsilon\right) = \qquad (28)$$

$$= \frac{\partial}{\partial x_j}\frac{\mu_t}{\sigma_\varepsilon}\frac{\partial \varepsilon}{\partial x_j} + C_{1\varepsilon}\frac{\varepsilon}{k}\left(P + (1 - C_{3\varepsilon})G\right) - C_{2\varepsilon}\rho\frac{\varepsilon^2}{k}$$

where $C_{1\varepsilon}$=1,44, $C_{2\varepsilon}$=1,92, $C_{3\varepsilon}$=1, σ_k = 1, σ_ε = 1,3 are constants determined based on empirical approach and $\sigma_h = \frac{\mu_t}{\lambda_t} c_p$ je Prandt's turbulent number.

A set of equations for transfer of scalar substance supplies the above-mentioned system of equations.

Static enthalpy equation: (see also formula 29)

$$\frac{\partial}{\partial t}\left(\rho \overline{h}\right) + \frac{\partial}{\partial x_j}\left(\rho \overline{u_j}\overline{h}\right) = \frac{\partial}{\partial x_j}\left[\left(\lambda + \lambda_t\right)\frac{\partial \overline{T}}{\partial x_j}\right] + \frac{d\overline{p}}{dt} + \tau_{jk}\frac{\partial \overline{u_j}}{\partial x_k} \quad (29)$$

Equation for additive mass fractions: (see also formula 28)

$$\frac{\partial}{\partial t}\left(\rho m_n\right) + \frac{\partial}{\partial x_j}\left(\rho \overline{u_j} m_n\right) = \frac{\partial}{\partial x_j}\left[\left(\rho D_{n,m} + \frac{\mu_t}{\delta_t}\right)\frac{\partial m_n}{\partial x_j}\right] \qquad (30)$$

where m_n is considered to be a mass ratio of compound in mixture, S_{ct} is Schmidt number and D_{nm} is diffusion coefficient for additive n in mixture.

Reynhold's tension values $\overline{u_i' u_j'}$ are via formula (31)

$$-\rho \overline{u_i' u_j'} = \mu_t \frac{\partial u_i}{\partial x_j} \qquad (31)$$

where the turbulent viscosity μt is supposed to be a function of length and speed measure with respect to Kolmogorov-Prandtl's hypothesis (see also formula (32),

$$\mu_t \approx l.\overline{v} = \rho C_\mu \frac{k^2}{\varepsilon} \qquad (32)$$

while the length measure values may be calculated with respect to formula (33)

$$l = C_\mu \frac{k^{2/3}}{\varepsilon} \qquad (33)$$

and the speed values may be calculated with respect to formula (34)

$$\sqrt{k} = \sqrt{\overline{u_j' u_j'}} \qquad (34)$$

Boussinesq's approximation

If a streaming is considered to be non-compressible and modeled based on this assumption as well a relation between density and temperature may be approximated based on Boussinesq's model. The density item contained in that model is considered to be constant or reference value, when providing solutions of all equations except upward pressure item contained within equation, which represents motion and may be replaced from formal point of view as follows:

$$\left(\rho - \rho_{ref}\right) g_i = -\rho_{ref}\beta\left(T - T_{ref}\right) g_i \qquad (35)$$

where the item ρ_{ref} represents reference density and the item T_{ref} is a temperature, while the item β is a thermal expansivity coefficient and the following formula may be postulated: $\rho = \rho_{ref}(1-\beta\Delta T)$. This approximation may be considered to be sufficient in the case of small changes in density values.

The momentum transfer equation within fluent environment is postulated via formula (36)

$$\frac{\partial}{\partial_t}\left(\rho \overline{u_i}\right) + \frac{\partial}{\partial x_j}\left(\rho \overline{u_i u_j}\right) = \frac{\partial}{\partial x_j}\left[\mu\left(\frac{\partial \overline{u_i}}{\partial x_j} + \frac{\partial \overline{u_j}}{\partial x_i}\right) - \left(\frac{2}{3}\mu\frac{\partial \overline{u_l}}{\partial x_l}\right)\right] \quad (36)$$

$$-\frac{\partial \overline{p}}{\partial x_i} + \rho g_i + F_i - \frac{\partial}{\partial x_j}\left(\rho \overline{u_i' u_j'}\right)$$

Volume : 4 | Issue : 2 | Feb 2014 | ISSN - 2249-555X

After the density differences $(\rho-\rho_{ref}).g_i$ becomes an integral part of the upward force item and the density value ρ is replaced by reference density value ρ_{ref} an equation for pressure p correction is postulated with respect to formula (37)

$$\frac{\partial}{\partial t}\left(\rho_{ref}\overline{u_i}\right)+\frac{\partial}{\partial x_j}\left(\rho_{ref}\overline{u_i}\,\overline{u_j}\right)= \quad (37)$$

$$=\frac{\partial}{\partial x_j}\left[\mu.\left(\frac{\partial\overline{u_i}}{\partial x_j}+\frac{\overline{u_j}}{\partial x_i}\right)-\left(\frac{2}{3}\mu\frac{\partial\overline{u_l}}{\partial x_l}\right)\right]-\frac{\partial\overline{p}^*}{\partial x_i}+$$

$$+\delta_{i3}\left(\rho-\rho_{ref}\right)g_i+F_i-\frac{\partial}{\partial x_j}\left(\rho\overline{u_i'u_j'}\right)$$

This equation may be received so that we make an addition and subtraction of the item $\rho_{ref}.g_i$ subsequently, while the item ρ_{ref} corresponds to formula

$$\rho_{ref}\,g_i=\frac{\partial\overline{p_{ref}}}{\partial x_i}$$ and p_{ref}

item is considered to be hydrostatic pressure, which corresponds to the reference density value ρ_{ref}.

As a result of the equation right side may be postulated as follows:

$$\ldots=\frac{\partial}{\partial x_j}\left[\mu.\left(\frac{\partial\overline{u_i}}{\partial x_j}+\frac{\partial\overline{u_j}}{\partial x_i}\right)-\left(\frac{2}{3}\mu\frac{\partial\overline{u_l}}{\partial x_l}\right)\right]-\frac{\partial\overline{p}}{\partial x_i}+$$

$$+\frac{\partial p_{ref}}{\partial x_i}-\frac{\partial p_{ref}}{\partial x_i}+\rho g_i+F_i-\frac{\partial}{\partial x_j}\left(\rho\overline{u_i'u_j'}\right)$$

$$\ldots=\frac{\partial}{\partial x_j}\left[\mu.\left(\frac{\partial\overline{u_i}}{\partial x_j}+\frac{\partial\overline{u_j}}{\partial x_i}\right)-\left(\frac{2}{3}\mu\frac{\partial\overline{u_l}}{\partial x_l}\right)\right]-\left(\frac{\partial\overline{p}}{\partial x_i}-\frac{\partial p_{ref}}{\partial x_i}\right)+$$

$$+\left(\rho-\rho_{ref}\right)g_1+F_i-\frac{\partial}{\partial x_j}\left(\rho\overline{u_i'u_j'}\right)$$

$$\frac{\partial\overline{p}}{\partial x_i}-\frac{\partial p_{ref}}{\partial x_i}=\frac{\partial p^*}{\partial x_i},$$

where p* is a difference between actual pressure p and hydrostatic pressure p_{ref}, which corresponds to reference density value ρ_{ref}.

THE RNG κ–ε MODEL

This model is derived based on classic κ–ε model, while a set of mathematics steps is applied there, which is denoted as the re-normalization group method. The re-normalization procedure or algorithm applied to turbulence is based on a subsequent eliminating of small whirlpools, while the motion (Navier-Stokes) equations, so that turbulent viscosity and force value together with non-linear items are being modified and transformed. If an appropriate assumption exists, which postulates that these whirlpools are related to dissipating ε, than turbulent viscosity values μ_t depend on turbulent whirlpools and the viscosity values may be calculated based on iterative removal of narrow zones, while an appropriate relation is applied in that iterative procedure. That construction approach may be selected when RNG method is being applied for these purposes.

$$\frac{d\mu_{eff}}{dl}=\frac{A_1\varepsilon l^3}{\mu(l)^2} \quad (38)$$

We may get equation (38), when integrating this equation with the use of length measure l, while an initial condition is defined as $\mu_{eff}=\mu_{mol}$ and the l measure postulates formula $l=l_d=L/Re^{3/4}$. This is considered to be the Kolmogor's dissipation measure, which corresponds to turbulent whirlpools.

$$\mu_{eff}(l)=\mu_{mol}\left[1+\frac{3A_1\varepsilon}{4\mu_{mol}^3}\left(l^4-l_d^4\right)\right]^{1/3} \qquad (l\geq l_d) \quad (39)$$

The equation (39) is considered to be an interpolation formula, when calculating value $\mu_{eff}(l)$ between molecular viscosity dispatching whirlpools viscosity with limit $l>>l_d$, which corresponds to high values of Reynolds's numbers. It is possible to present a proof that equation (39) may correspond to formula (40).

$$\mu_{eff}\approx\mu_t=(0{,}094l)^2\left|\nabla\overline{u}\right| \quad (40)$$

That conclusion corresponds to Prandtl's classical theory of blending or mixing layer derived based on an appropriate experiment. If the kinetic energy contained within internal whirlpool area (the measure is less than L is equal $k=0.71\varepsilon^{2/3}L^{2/3}$), than the formulas for whirlpool viscosity calculation may be derived based on principles representing analogy related to κ–ε model.

$$\mu_t=\rho C_\mu\frac{k^2}{\varepsilon} \quad C\mu=0{,}\mathbf{9} \quad (41)$$

However, the equation (39) may be simplified to algebraic dependence κ and ε

$$\mu_{eff}=\mu_{mol}\left[1+\sqrt{\frac{C_\mu}{\mu_{mol}}}\frac{k}{\sqrt{\varepsilon}}\right]^2 \quad (42)$$

The RNG κ–ε Model derived with the use of statistic averaging method has the form, formal point of view. The motivity transfer equation may be postulated with respect to formula (43).

$$\frac{\partial}{\partial t}\left(\rho\overline{u_i}\right)+\frac{\partial}{\partial x_j}\left(\rho\overline{u_i}\,\overline{u_j}\right)= \quad (43)$$

$$=\frac{\partial}{\partial x_j}\left(\mu_{eff}\left[\frac{\partial\overline{u_i}}{\partial x_j}+\frac{\partial\overline{u_j}}{\partial x_i}\right]-\left(\frac{2}{3}\mu_{eff}\frac{\partial\overline{u_l}}{\partial x_l}\right)\right)-\frac{\partial\overline{p}}{\partial x_i}+\rho g_i+F_i$$

The viscosity for high Reynolds's number is being calculated based on formula (39) and for low Reynolds's number is being calculated based on formula (40). The transport equations for κ and ε correspond to formulas (44 and 45)

$$\frac{\partial}{\partial t}(\rho k)+\frac{\partial}{\partial x_j}\left(\rho\overline{u_j}k\right)=\frac{\partial}{\partial x_j}\left(\alpha_k\mu_{eff}\frac{\partial k}{\partial x_j}\right)+\mu_tS^2-\boldsymbol{\rho} \quad (44)$$

$$\frac{\partial}{\partial t}(\boldsymbol{\rho}\ )+\frac{\partial}{\partial x_j}\left(\rho u_j\varepsilon\right)=\frac{\partial}{\partial x_j}\left(\alpha_\varepsilon\mu_{eff}\frac{\partial\varepsilon}{\partial x_j}\right)+ \quad (45)$$

$$+C_{1\varepsilon}\frac{\varepsilon}{k}\mu_tS^2-C_{2\varepsilon}\rho\frac{\varepsilon^2}{k}-R$$

where α_κ and α_ε are considered to be inverse Prandtl's numbers for turbulent energy dissipation and are derived based on RNG theory and postulated via formulas (46 – 50).

$$\left|\frac{\alpha-1{,}3929}{\alpha_0-1{,}3929}\right|^{0{,}6321}\left|\frac{\alpha+2{,}3929}{\alpha_0+2{,}3929}\right|^{0{,}3679}=\frac{\mu_{mol}}{\mu_{eff}},\alpha_0=1 \quad (46)$$

and the R-item is postulated via formula (46)

$$R=v_TS_j\frac{\partial\overline{u_l}}{\partial x_i}\frac{\partial\overline{u_l}}{\partial x_j} \quad (47)$$

and it enables postulating formula (48) for model RNG

$$R=\frac{C_\mu\rho\eta^3\left(1-\eta/\eta_0\right)}{1+\beta\eta^3}\frac{\varepsilon^2}{k} \quad (48)$$

while

$$\eta=S\frac{k}{\varepsilon} \quad \text{and} \quad S^2=2S_{ij}S_j \quad (49)$$

and

$$S_{ij}=\frac{\partial\overline{u_i}}{\partial x_j}\frac{\partial\overline{u_j}}{\partial x_i} \quad (50)$$

The equations (46-50) represent a modified RNG κ–ε model, which contains postulated constants: $C_{\varepsilon1}=1.42$; $C_{\varepsilon2}=1.68$; α_P

Volume : 4 | Issue : 2 | Feb 2014 | ISSN - 2249-555X

= 1.39. However, the model may be refined further as well.

Near wall modeling, wall function

Near wall modeling, wall function is being affected through numeric solution precision within entire area. The items to be investigated are being changed very rapidly, when considering situation closed to the wall. The momentum or motility transfer and a transfer of other scalar values are applied there in a great deal. Turbulence effects are suppressed closed the wall, however a considerable level of turbulent kinetic energy is observed in the external part of a bordering layer, as a result of Reynolds tensions and medium speed gradient. The area closed the wall denoted as bordering layer may be divided into several parts. This fact was confirmed based on more experiments provided related to this objective.

The *viscose (laminar) sub-layer* is located primary near the wall, while streaming is considered to be almost laminar and molecular viscosity has a dominant effect related to dynamics, heat and mass transfer. A bordering layer outer part is considered to *fully turbulent layer*, while turbulence plays a role of dominant importance there.

The *transient layer* is located between laminar and fully turbulent layer, where the molecular viscosity a turbulence effects are applied in the same measure. Figure 2 shows the bordering layer distribution.

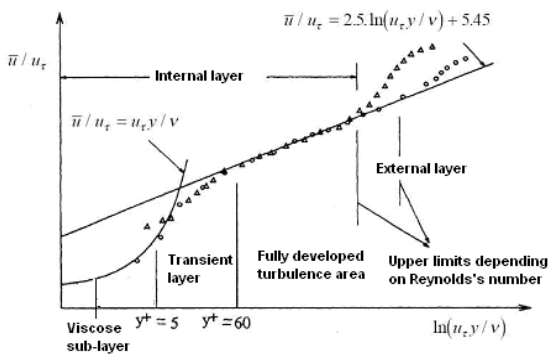

Figure 2: The near-wall area distribution

Two different approaches may applied, when providing near-wall modeling The first approach is based on the wall function definition, which enables to overcome the laminar sub-layer and transient layer, where the molecular and turbulent viscosity is effect is observed. This area is located between wall and fully developed turbulent streaming. The second approach is based on a detailed near-wall modeling, incl. the sub-layer closely related to a fine grid. Fig.3 shows the basic principles concerned to both of the above-mentioned approaches.

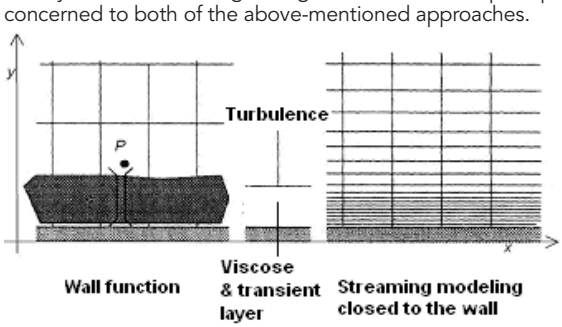

Figure 3: Near-wall modeling grid creation

If the wall function is applied for streaming, where a large value of Reynolds's number is observed, the calculation demands become lower. It means, a calculation precision is sufficient and efficient from economic point of view and is considered to be a suitable solution for most of engineering problems, as a result of that. The wall functions include the media speed and temperature wall law together with appropriate quantitative relations for near-wall turbulence items.

Thermocouple

This type of thermocouple sensor is not made based on standard materials and the sensor alone cannot be considered to be standard or classic thermocouple sensors, as a result of that. It is not necessary to work with an entire sensor for these purposes, however it is sufficient to take only that part, which is located in the burn gas pipe and has a direct contact with an appropriate flowing liquid. Table 1 contains information concerned to material composition for that part of thermocouple only.

Table 1 Material composition and physical properties of the temperature scanner (c – thermal capacity, k – thermal conductivity, ρ - density, E - Young's modulus, α- thermal expansivity coefficient.

Design element	Material	c [J/kg.K]	k [W/m.K]
Thermocouple wires	Chromel P (10% Cr)	428	33
Thermoball	X2 Cr Ni MoN	500	15
Sensor cover	Ni Cr 28 Fe Si C	500	21
Cover intermediate space fill	MgO	600	42
Sealing ring, protective roll	Steel 17 242	501	14,6
Design element	p [kg/m^3]	E [Pa]	α [1/K]
Thermocouple wires	8730		
Thermoball	8000		
Sensor cover	8000		
Cover intermediate space fill	3580	2,5.10^{11}	1,08.10^{-5}
Sealing ring, protective roll	7800		

Six volumes were created based on 3D model (see also figure 4), while they represented parts postulated as follows: thermocouple, sensor cover, sensor and thermocouple intermediate space filling, protective roll, sealing ring and liquid. Figure 5 shows the thermocouple protective model cover.

The model has been filled with cross-linked tetrahedral elements, the number of which is 5.75 million, while the smallest volume was 1.65.10^{-9} mm3. After having postulated the bordering conditions, the model solution was done based on assumption that, the model was considered to be non-stationary and times depend. Figure 6 shows burning gas input into the pipe through the blue color surface and burn gas output. Figure 7 shows the surface network of appropriate parts. Figure 8 shows a section through pipe tetrahedral network across the thermocouple. However, the same figure contains an image concerned to details of thermocouple wires as well. Figure 9 shows a model of thermocouple measuring part, while a yellow line is lying in a parallel direction to pipe axis and the temperature values related to figure 13 and figure 14. The co-ordinates (0, 0, 0) represent a position of the thermocouple-measuring ball.

Calculation of limit conditions

The simulation calculation has been applied, in order to find the time needed for heating of the sensor ball to achieve required temperature. An input liquid initial temperature was 500 K together with a complete model. A calculation has been started after calculation numeric stabilizing, when the temperature was set to 900 K. A flowing speed and operating pressure values were the same in the case of stabilized calculation (liquid input speed 60 m.s^{-1} and pressure 101325 Pa). A length of pipe, in the middle of which the thermo-

Volume : 4 | Issue : 2 | Feb 2014 | ISSN - 2249-555X

couple was installed, was 100 m. Non-stationary calculation time step was 2 seconds for 20 iterations per one time step. The simulation process was running in 55 time steps. A set of values closely related to material properties applied for calculation purposes is contained in Table 1. The flow stabilization after thermocouple was achieved in 12th second of calculation running, after temperature step change. This is a reason why the flow and temperature image is closely related to 12 seconds after temperature step change.

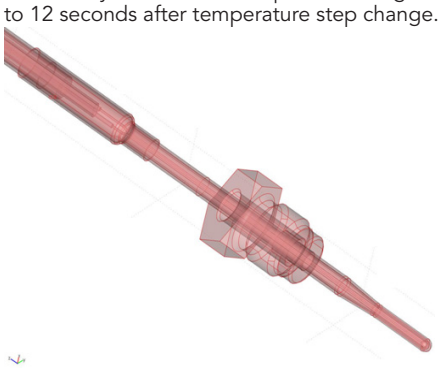

Figure 4: Temperature sensor- three dimensional model

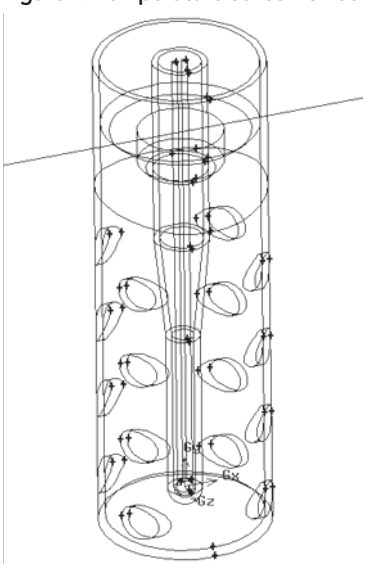

Figure 5: A model of sensor part covered by protective roll with holes located in pipe

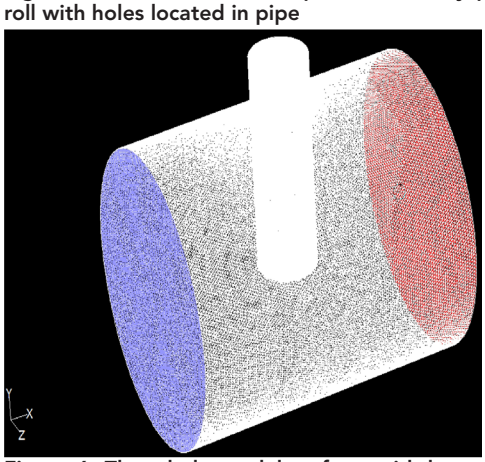

Figure 6: The whole model surface grid, burn gas input (blue), burn gas output (red).

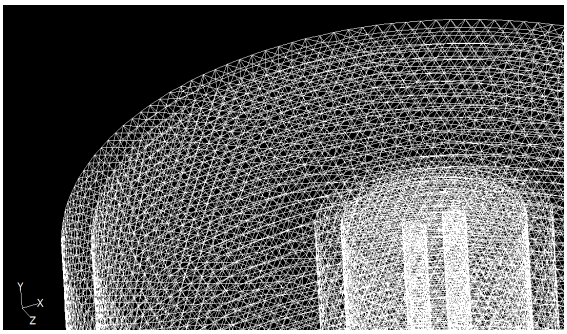

Figure 7: The whole model surface grid, burn gas input (blue), burn gas output (red).

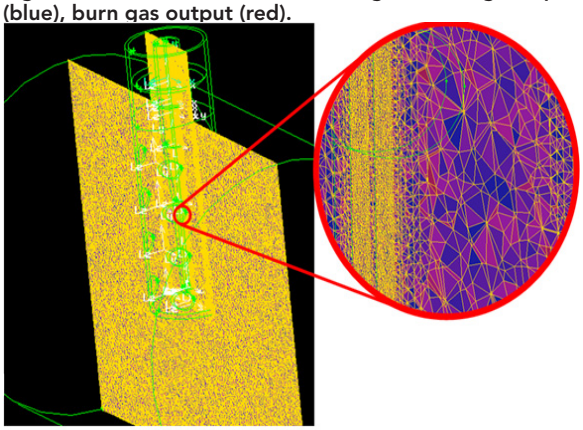

Figure 8: Model network section – thermocouple wires visualized via to vertical bands having the thickest networking (detailed image)

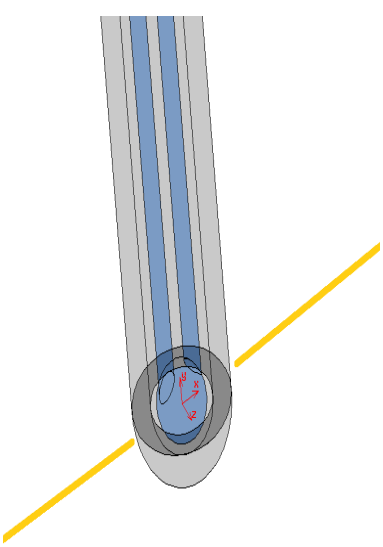

Figure 9: Thermocouple measuring part model x-blowing direction

Figure 10 and figure 11 show a temperature field in 2 sections in time of 12 seconds after temperature step change. When looking at these figures, you can see a distribution of temperature values within thermocouple and its neighborhood. Figure 12 shows a speed field via set of speed vectors, where you can see an effect of pipe with holes related to flowing in the sensor neighborhood. A temperature of thermocouple measuring ball was measured, so that the yellow line temperature values were visualized, which is parallel to pipe axis (see also figure 9) and the thermocouple ball temperature value was taken from graph in time when calcula-

Volume : 4 | Issue : 2 | Feb 2014 | ISSN - 2249-555X

tion was running (see also figure 13). The resulting graph was created based on the results, while that graph is shown in figure 14.

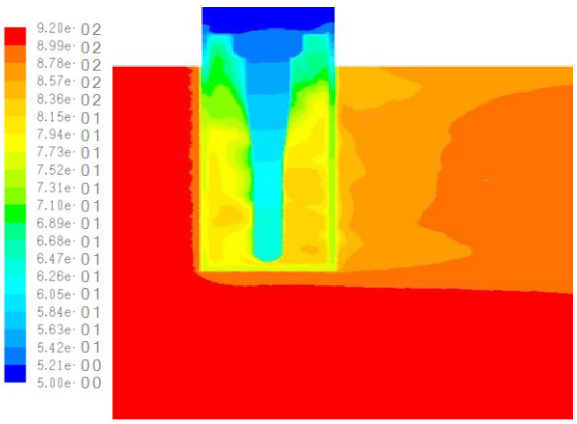

Figure 10: Temperature field (K), axial section along pipe axis, time 12 seconds

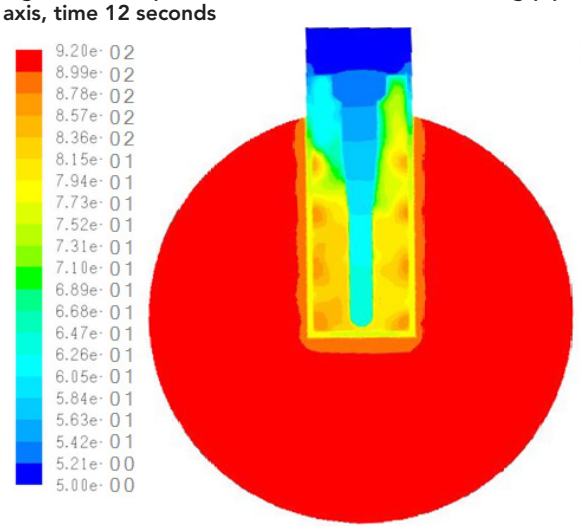

Figure 11: Temperature field (K), axial section perpendicular to pipe axis, time 12 seconds

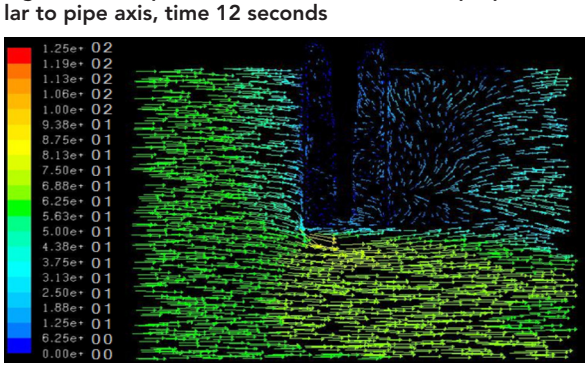

Figure 12: Speed vectors (m.s-1), axial section within pipe axis, time 12 seconds after starting temperature step change.

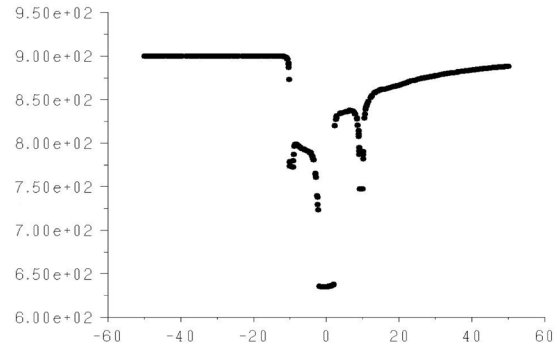

Figure 13: A relation between temperature (K) and thermocouple distance (mm), in the pipe axis, 12 minutes after temperature step change. The visualized temperature values are lying on a yellow line with respect to figure 9.

When looking at figure 14, you can see a slow change of temperature related to thermocouple ball. This heating speed is affected via thermocouple construction material and a nature of flowing round the thermocouple. You can see it better in Fig. 14, position 0 indicates a thermocouple on x, - 50 mm is the temperature of ingoing gas products +50 is the temperature of outgoing gas products.

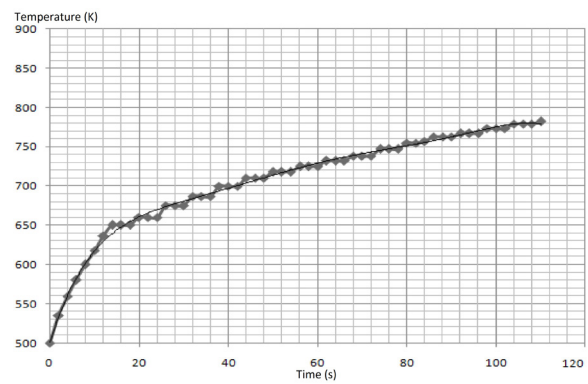

Figure 14: Thermocouple measuring ball temperature versus time beginning from temperature step change

Conclusion

The simulation calculation was applied in order to show a possibility concerned to investigation of thermocouple response speed with respect to flow medium temperature step change. The materials CrNi, steel, MgO have a low thermal conductivity and the protective pipe makes a heating speed worse. The CFD method may be applied in order to optimize a number of holes in a protective pipe and their arrangement with respect to flowing and to test selection of materials, when preparing proposal concerned to thermocouple design.

Acknowledgements

This publication is the result of the project implementation. The project name is „Autonomous robust mechatronic systems for ultra deep geothermal boreholes. " ITMS code 26220220139, supported by the Research & Development Operational Programme funded by the European Regional Development Fund.

Volume : 4 | Issue : 2 | Feb 2014 | ISSN - 2249-555X

European Regional Development Fund:

The Agency of the Ministry of Education, Science, Research

Operational Programme Research and Development:

REFERENCE

[1] SCHŰTZ, P. 2011: Simulácia odozvy snímača teploty na parametre prudiacej tekutiny, Diploma thesis, Strojnícka fakulta, Žilinská univerzita v Žiline, | [2] VERSTEEG, H. K. – Malalasekera W.: An Introduction to COMPUTATIONAL FLUID DYNAMICS, The finite Volume Method - second edition, Pearson Education Limited 1995, 2007, ISBN 978-0-13-127498-3, 308s. | [3] BAEHR, H. D. – STEPHAN, K.: Heat and Mass Transfer, Second revised Edition, Springer Berlin Heidelberg New York, ISBN -10 3-540-29526-7, 670s | [4] LIENHARD IV, J. H. – LIENHARD V, J. H.: A heat transfer textbook, Third Edition, Phlogiston Press Cambridge, Massachusetts, 2008 | [5] KOZUBKOVÁ, M. – DRÁBKOVÁ, S.: Numerické modelování proudení, Fluent I, Vysoká škola báňská - technická univerzita Ostrava, 2003 | [6] LÁBAJ, J.: Spaľovanie a plameň. Knižné centrum v Žiline 2002,., ISBN 80-8064-135-8, 166 s | [7] DRDOL, K. – SOKOL, M. 2013: The impact of design parameters to change the cutting chamber performance crushing device, In: TRANSCOM 2013: 10-th European conference of young research and scientific workers: Žilina, June 24-26, 2013, Slovak Republic. - Žilina: University of Žilina. - ISBN 978-80-554-0695-4. - S. 75-78. | [8] KAMAS, P. – DRDOL, K. 2013: Working cycle design of movement-anchoring mechanism in deep drilling, TRANSCOM 2013: 10-th European conference of young research and scientific workers: Žilina, June 24-26, 2013, Slovak Republic. - Žilina: University of Žilina, - p. 161-164 ISBN 978-80-554-0695-4. | [9] ŽARNAY, M. – SOKOL, M. 2013: Experimental device for testing of the functional design of plazmabit movement-anchoring system / Technológ : časopis pre teóriu a prax mechanických technológií. - Roč. 5, č. 3 (2013), p. 71-76. - ISSN 1337-8996. |